Supplementary Information

Pd_3Bi intermetallic particles prepared by photodeposition method for photocatalytic ethane production from methane

Surya Pratap Singh,[a] Kosuke Beppu,[a] and Fumiaki Amano*[a]

[a]Department of Applied Chemistry for Environment, Faculty and Graduate School of Urban Environmental Sciences, Tokyo Metropolitan University, 1-1, Minami-Osawa, Hachioji, Tokyo 192-0397.

*Corresponding author

Fumiaki Amano: f.amano@tmu.ac.jp

S1. Experimental

S1.1 Materials

The following chemicals were used as received without further purification. Gallium oxide (Kojundo Chemicals, GA004PB, 99.99%), a Pd standard solution ($Pd(NO_3)_2$ in 6.6 mol L^{-1} HNO_3 (aq.) containing 5 mg mL^{-1} Pd, Wako Chemicals), a Bi standard solution ($Bi(NO_3)_3$ in 0.5 mol L^{-1} HNO_3 (aq.) containing 1 g L^{-1} Bi, Wako Chemicals), methanol (Wako Chemicals, 99.8%), Silica gel (CARiACT G-3, Fuji Silysia Chemical Ltd), 5,5-dimethyl-1-pyrroline *N*-oxide (DMPO).

CH_4 (Taiyo Nippon Sanso, 99.999% pure) was used as a reactant. Ar (Taiyo Nippon Sanso, 99.9975% pure) and He (Japan Helium Centre Corporation, 99.995% pure) were used as the carrier gases for the two gas chromatographs (GC) equipped with thermal conductivity detectors (TCD). N_2 (Taiyo Nippon Sanso, 99.998% pure) was used as a carrier gas for the GC equipped with a flame ionization detector (FID). H_2 (Keiyo Gas Company, 99.99% pure) along with air (from an air compressor, Hitachi) were used to make a flame in the GC-FID.

S1.2 Methods

S1.2.1 Catalysts preparation

S1.2.1.1 Deposition of Pd-Bi cocatalysts by the simultaneous photodeposition method

The Pd-Bi cocatalysts were loaded on the gallium oxide (Ga_2O_3) sample by a simultaneous photodeposition method under UV irradiation. A schematic overview is shown in Fig. S1. A detailed procedure is as follows. 1.0 g of Ga_2O_3 was dispersed in 100 mL of 10% methanol aqueous solution. This suspension was ultrasonicated for 5 min. Next, 0.2 mL of Pd standard solution and 2 mL of Bi standard solution were added to the above suspension. After ultrasonication for 5 min, the above suspension was stirred for 25 min in dark and subsequently irradiated by a 40 W low-pressure mercury lamp (ASM401N, Asumi Giken) for 1h under stirring. Then, the obtained powder was filtered, washed with deionized water 7 to 10 times, centrifuged, dried at 353 K overnight and collected. Thus prepared sample was referred to as Pd-Bi(PD)/Ga_2O_3; where the theoretical loading amount of Pd and Bi was 0.1 and 0.2 wt.%, respectively. The Pd/Bi ratio is 1.

S1.2.1.2 Deposition of single Pd and Bi cocatalysts by the photodeposition method

The single Pd and Bi cocatalyst-loaded Ga_2O_3 samples were prepared by a photodeposition method under UV irradiation. The procedure was the same as that for the simultaneous photodeposition except that only one precursor standard solution was added. Thus prepared samples were referred to as Pd(PD)/Ga_2O_3 and Bi(PD)/Ga_2O_3; where the loading amount of Pd and Bi was 0.1 and 0.2 wt.% in the first and second samples, respectively.

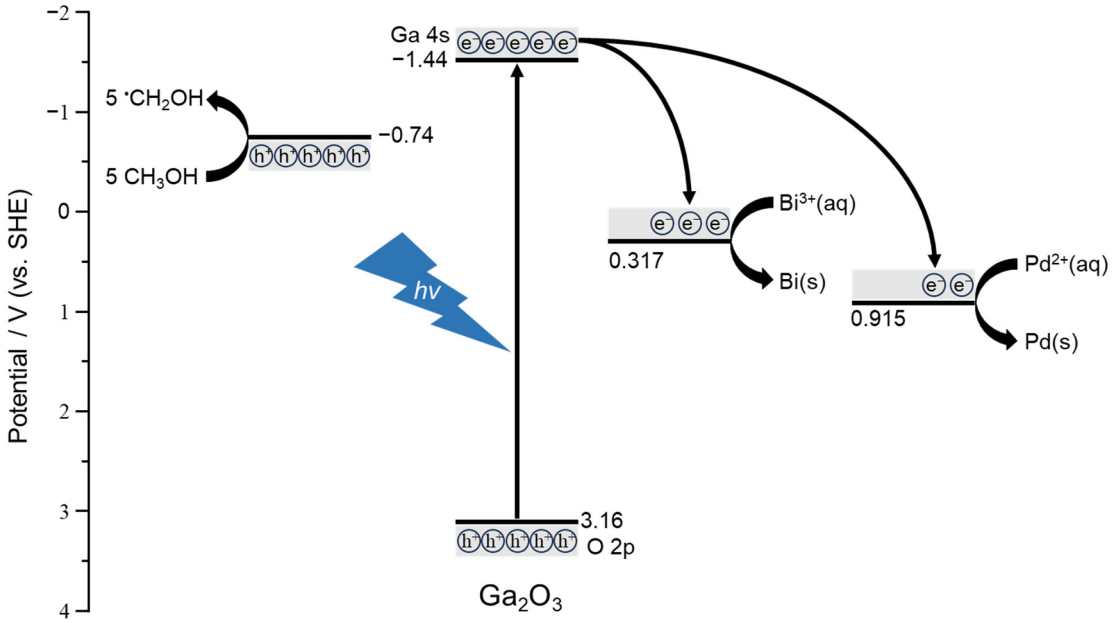

Fig. S1 Schematic overview of photodeposition method for depositing Pd and Bi on Ga_2O_3 surface using methanol as a sacrificial electron donor. The photogenerated electrons reduce the metal salt (M^{n+}) to metallic particles: $M^{n+}(aq) + ne^- \rightarrow M(s)$.

S1.2.1.3 Deposition of Pd-Bi cocatalysts by the co-impregnation method

For comparison, the Pd-Bi cocatalysts were loaded on the Ga_2O_3 by a co-impregnation method. The detailed procedure is as follows. 1.0 g of Ga_2O_3 was dispersed in 100 mL of deionized water. This suspension was ultrasonicated for 5 min. Next, 0.2 mL of Pd standard solution and 2 mL of Bi standard solution were added to the above suspension. After ultrasonication for 5 min, the above suspension was stirred in the dark for 25 min. Subsequently, the suspension was heated at 353 K under stirring to evaporate water to dryness. The obtained

powder was dried at 353 K overnight and calcined in air at 773 K for 3 h. Thus prepared sample was referred to as Pd-Bi(IMP)/Ga_2O_3; where the loading amount of Pd and Bi was 0.1 and 0.2 wt.%, respectively (Pd/Bi ratio = 1).

S1.2.1.4 Hydrogen treatment of Pd-Bi(IMP)/Ga_2O_3 at elevated temperatures

The Pd-Bi(IMP)/Ga_2O_3 sample was reduced in a flow of hydrogen (100 mL min^{-1}) at 373, 473, 673 and 973 K for 1 h. Thus prepared samples were referred to as Pd-Bi(IMP-373R)/Ga_2O_3, Pd-Bi(IMP-473R)/Ga_2O_3, Pd-Bi(IMP-673R)/Ga_2O_3 and Pd-Bi(IMP-973R)/Ga_2O_3, respectively.

S1.2.1.5 Preparation of Pd_3Bi/SiO_2 and Pd/SiO_2

Pd_3Bi/SiO_2 were synthesized by sequential impregnation method and subsequent hydrogen reduction following the procedure described in the literature [*ACS Catal.*, 2022, 10531–10545]. The detailed procedure is as follows. Aqueous ammonia solution was added to 4.2 mL of Pd standard solution until the pH became 11. Then this solution was added to 1.0 g of silica gel dropwise with continuous stirring, evaporated at 353 K and dried overnight. Then the powder was calcined at 673 K for 3 h to give the Pd(IMP)/SiO_2. Next, 10.1 mL of Bi standard solution was added to 0.5 g of Pd(IMP)/SiO_2 powder, evaporated at 353 K and dried overnight. The obtained powder was calcined at 673 K for 4 h, and reduced in hydrogen atmosphere (100 mL min^{-1}) at 473 K for 30 min followed by 823 K for 30 min. This sample is referred to as Pd_3Bi/SiO_2 for simplification. The loading amount of Pd and Bi each was 2 wt.% (Pd/Bi ratio = 2). A sample with higher loading amount (10 wt.% each) was also prepared following the same procedure.

The Pd(IMP-673R)/SiO_2 sample was prepared by the impregnation method. Aqueous ammonia solution was added to 4.2 mL of Pd standard solution until the pH became 11. Then this solution was added to 1.0 g of silica gel dropwise with continuous stirring, evaporated at 353 K, and dried overnight. Then the powder was calcined at 673 K for 3 h to give the Pd(IMP)/SiO_2. Then, the powder was reduced in a hydrogen atmosphere (100 mL min^{-1}) at 673 K for 2 h. The loading amount of Pd was 2 wt.%. A sample with higher loading amount (10 wt.%) was also prepared following the same procedure

S1.2.2 Characterization

The photocatalyst samples were characterized by several techniques. The actual loading amounts of the cocatalysts were determined by the inductively coupled plasma atomic emission spectroscopy (ICP-AES) using a Shimadzu ICPE-9820 plasma atomic emission spectrometer. The samples were dissolved in aqua regia and diluted with deionized water for the measurement. The crystal structure was determined by the powder X-ray diffraction (XRD) using a Rigaku SmartLab X-ray diffractometer with Cu K_α radiation (40 kV, 30 mA). The optical properties of the samples were measured by the diffuse reflectance ultraviolet-visible (DR UV-vis) spectroscopy using a Shimadzu UV-2600 UV-vis spectrophotometer with an ISR-2600Plus integrating sphere using barium sulfate powder as a reference. The scanning electron microscope (SEM) images were recorded on a JEOL JSM-7500F field emission scanning electron microscope. A compositional mode in retractable backscattered electron imaging (RBEI) was used to visualize the cocatalyst nanoparticles based on elemental contrast difference. The transmission electron microscope (TEM) and scanning transmission electron microscope (STEM) images with energy dispersive X-ray (EDX) mappings were recorded using a JEOL JEM-ARM200F NEOARM atomic resolution analytical electron microscope. Pd K-edge X-ray absorption fine structure (XAFS) was measured at BL01B1 and NW10A beamlines of the synchrotron radiation facilities, SPring-8 and Photon Factory (PF), respectively, in fluorescence mode using a 19-element germanium solid state detector (19 Ge SSD). The Athena program was used to analyse the obtained XAFS data. Artemis program was used for the fitting of XAFS data. MorletE program was used to make the Wavelet transform of the XAFS data. Electron spin resonance (ESR) spectra were measured using a Bruker ESR5000 spectrometer with DMPO as a spin-trapping scavenger in the aqueous suspension of photocatalyst powders.

S1.2.3 Photocatalytic reaction setup and product analysis

The reaction tests of the photocatalytic methane conversion with the water vapour were performed in a fixed bed flow reactor (volume = 5 × 5 × 0.025 cm^3). We spread 50 mg of the photocatalyst sample powder onto a glass plate covering an area of 25 (5 × 5) cm^2 with the help of deionized water, then it was dried at room temperature overnight. Subsequently, this photocatalyst-coated glass plate along with the quartz window plate was sandwiched between two stainless-steel plates to assemble the reactor (Fig. S2). 20 mL min^{-1} of the pure methane was bubbled in a glass cylinder containing deionized water at room temperature and

atmosphere pressure. The resulting mixture of pure methane gas and water vapour was introduced to the reactor. Water vapour pressure (P_{H2O}) in the gas stream was measured in the range of 2.9–3.2 kPa by a dew point meter (EE3 hygrometer, Tekhne) installed in the streamline. The photocatalyst (irradiation area 25 cm^2) was irradiated by a 40 W low-pressure mercury lamp (ASM401N, Asumi Giken) held above the reactor. The intensity of the light measured by a Hamamatsu UV Power Meter C9536/H9535 at the wavelength of 254 nm was approximately 14 mW cm^{-2}. The reactor temperature was controlled to be 298 K by an electronic cooler (HMC-17F-2700, Hayashi Clock Industry) but increased by about 2–4 K measured by a thermocouple during the photoirradiation. The outlet gases were analysed by the gas chromatographs equipped with a thermal conductivity detector (GC-TCD, Shimadzu GC-8A) and flame ionization detector (GC-FID, Shimadzu GC-2025). The GC-TCD with the argon carrier using a packed column (Molecular Sieves 5A) was used to quantify hydrogen and oxygen. The GC-TCD with the helium carrier gas using a packed column (Shincarbon ST) was used to quantify the carbon monoxide and carbon dioxide. The GC-FID with the nitrogen carrier gas using a capillary column (PoraBOND Q) was used to quantify the hydrocarbons (ethene, ethane, and propane).

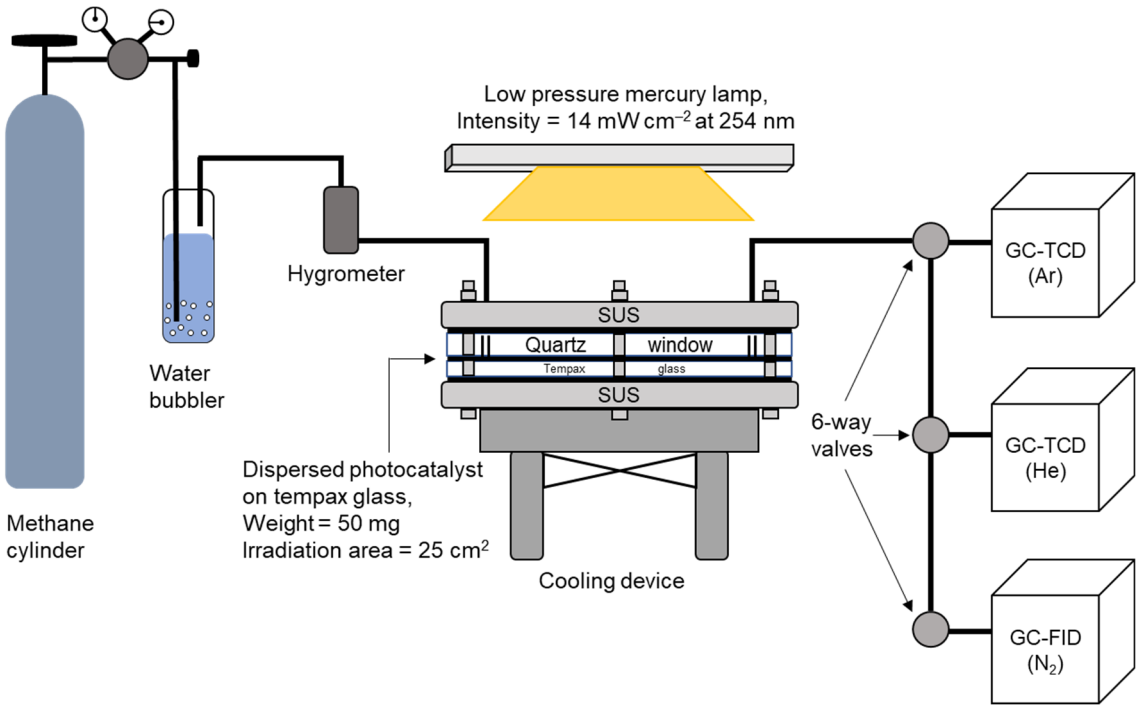

Fig. S2 Reaction set-up for the photocatalytic methane conversion with water vapour

S1.3 Calculations

S1.3.1 Selectivity

The selectivity of various products based on the carbon was calculated as shown in the following equations.

$$S_{C_2H_6}\,(\%) = \frac{2R_{C_2H_6}}{2R_{C_2H_6} + R_{CO_2} + R_{CO} + 3R_{C_3H_8} + 2R_{C_2H_4}} \times 100$$

$$S_{C_2H_4}\,(\%) = \frac{2R_{C_2H_4}}{2R_{C_2H_6} + R_{CO_2} + R_{CO} + 3R_{C_3H_8} + 2R_{C_2H_4}} \times 100$$

$$S_{CO_2}\,(\%) = \frac{R_{CO_2}}{2R_{C_2H_6} + R_{CO_2} + R_{CO} + 3R_{C_3H_8} + 2R_{C_2H_4}} \times 100$$

$$S_{CO}\,(\%) = \frac{2R_{CO}}{2R_{C_2H_6} + R_{CO_2} + R_{CO} + 3R_{C_3H_8} + 2R_{C_2H_4}} \times 100$$

where; R_x is the formation rate of product x, and S_x (%) is the selectivity of product x.

S1.3.2 Material balance

The material balance is calculated as the ratio of the hole (h^+) and electron (e^-) consumption in the photocatalytic reaction test by the following equation. The ideal h^+/ e^- ratio is 1.

$$\frac{h^+}{e^-} = \frac{R_{C_2H_6} + 4R_{CO_2} + 3R_{CO} + 2R_{O_2} + 2R_{C_3H_8} + 2R_{C_2H_4}}{R_{H_2}}$$

where; R_x is the formation rate of product x.

S1.3.3 Apparent quantum efficiency (AQE)

The apparent quantum efficiency (AQE) of hydrogen and ethane formation was calculated by the following equation.

$$\text{AQE (\%)} = \frac{R_\text{p} n_\text{e} N_\text{A}}{\frac{I_0 A \times 60(\text{s min}^{-1})}{hc/\lambda}} \times 100$$

where R_p is the formation rate of product (H_2 or C_2H_6, in mol min^{-1}), n_e is the number of electrons involved in the product formation (2 for H_2 and C_2H_6 formation), N_A is Avogadro constant (6.022×10^{23} mol^{-1}), I_0 is irradiance (0.014 W cm^{-2}), A is irradiation area (25 cm^2), h is Planck constant (6.626×10^{-34} J s), c is speed of light (3.0×10^8 m s^{-1}) and λ is wavelength of incident light (254×10^{-9} m).

S1.3.4 Methane conversion

The methane conversion was calculated as the ratio of moles of methane consumed to the moles of methane introduced in the feed gas according to the following equations.

$$\text{CH}_4 \text{ conversion (\%)} = \frac{\text{Moles of CH}_4 \text{ consumed}}{\text{Moles of CH}_4 \text{ fed}} \times 100$$

S2. Mechanism of product formation in photocatalytic methane conversion with water vapour

In our previous study (*Energy Fuels* 2022, 36, 5393−5402), •OH formation was observed in the Pd-loaded Ga_2O_3 photocatalyst using the ESR spin trapping technique. We proposed the mechanism for the photocatalytic ethane formation from methane in the presence of water vapour. Photogenerated hole (h^+) oxidizes water to form •OH, which activates methane to produce methyl radicals. The coupling of methyl radicals induces C_2H_6 formation. This •OH-mediated reaction mechanism differs from the photocatalytic non-oxidative coupling of methane (NOCM) performed in the absence of oxidants (e.g., *Catal. Today*, 2021, **375**, 264–272 and *ACS Catal.*, 2021, **11**, 13768–13781). Photoexcited electrons induce hydrogen evolution reaction.

$$Ga_2O_3 + h\nu \rightarrow e^- + h^+$$

$$2H^+ + 2e^- \rightarrow H_2$$

$$H_2O + h^+ \rightarrow {}^\bullet OH + H^+$$

$${}^\bullet OH + CH_4 \rightarrow {}^\bullet CH_3 + H_2O$$

$${}^\bullet CH_3 + {}^\bullet CH_3 \rightarrow C_2H_6$$

S3. Results of characterization

S3.1 Actual loading amounts of Pd and Bi

The actual loading amounts of Pd and Bi determined by ICP-AES are given in Table S1. Both Pd and Bi were almost completely loaded in all the samples.

Table S1 Loading amounts of Pd and Bi of the prepared photocatalyst samples determined by ICP-AES

Entry	Sample	Loading amount (wt.%)			
		Pd		Bi	
		Calculated	Measured*	Calculated	Measured*
1	Pd(PD)/Ga_2O_3	0.1	0.07	–	–
2	Bi(PD)/Ga_2O_3	–	–	0.2	0.17
3	Pd-Bi(PD)/Ga_2O_3	0.1	0.07	0.2	0.16
4	Pd-Bi(IMP)/Ga_2O_3	0.1	0.08	0.2	0.18
5	Pd-Bi(IMP-373R)/Ga_2O_3	0.1	0.08	0.2	0.21
6	Pd-Bi(IMP-473R)/Ga_2O_3	0.1	0.07	0.2	0.18
7	Pd-Bi(IMP-673R)/Ga_2O_3	0.1	0.08	0.2	0.18
8	Pd-Bi(IMP-973R)/Ga_2O_3	0.1	0.08	0.2	0.18

*Measured by ICP-AES. Calibration curves using standard solutions of Pd and Bi of various concentrations were made.

S3.2 XRD patterns

The XRD patterns of references (β-Ga_2O_3 and α-Ga_2O_3) and Ga_2O_3 powder, Pd(PD)/Ga_2O_3, Bi(PD)/Ga_2O_3, and Pd-Bi(PD)/Ga_2O_3 samples are given in Fig. S3.

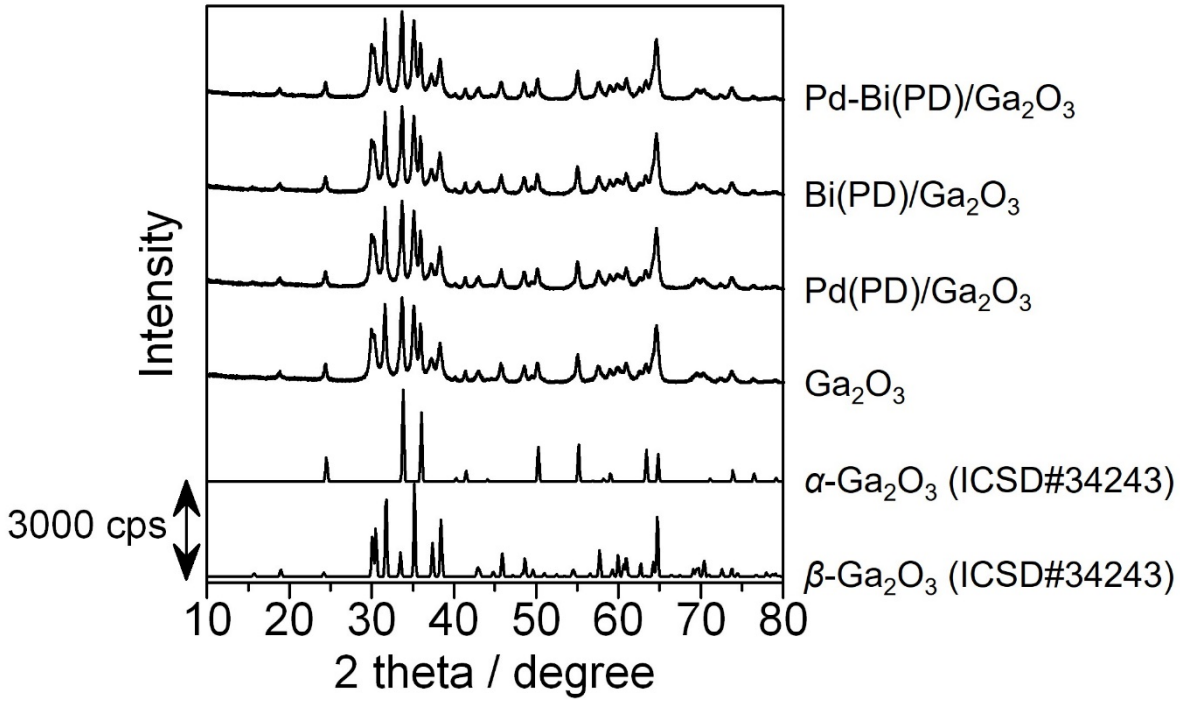

Fig. S3 XRD patterns of Ga_2O_3, Pd(PD)/Ga_2O_3, Bi(PD)/Ga_2O_3, and Pd-Bi(PD)/Ga_2O_3 samples and references.

S3.3 SEM images and particle size distributions

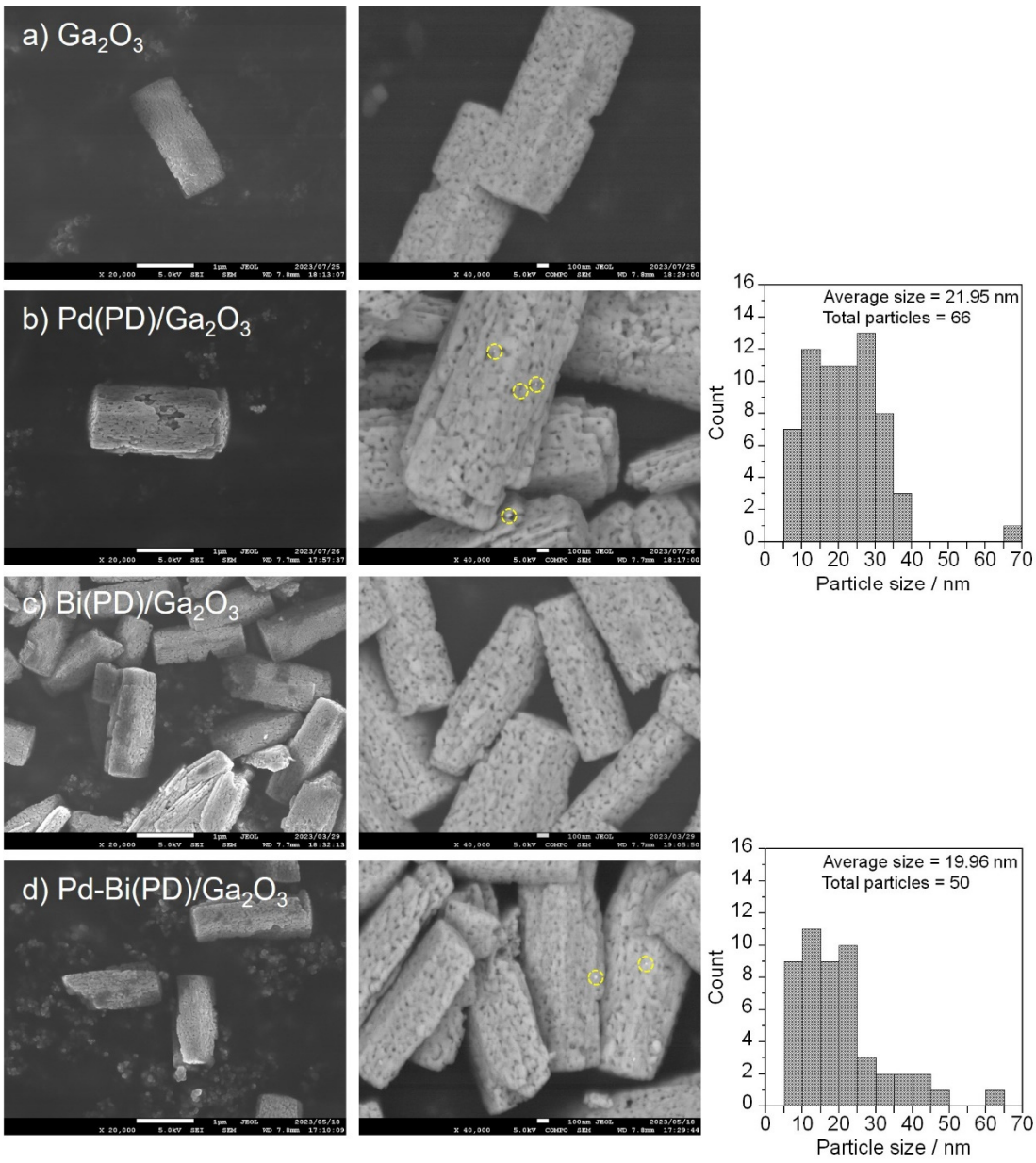

Fig. S4 Conventional SEM images (left), compositional SEM image (middle), and particle size distribution (right) for (a) Ga_2O_3, (b) $Pd(PD)/Ga_2O_3$, (c) $Bi(PD)/Ga_2O_3$, and (d) $Pd\text{-}Bi(PD)/Ga_2O_3$.The bright dots are encircled in the compositional images.

SEM images of Ga_2O_3, Pd(PD)/Ga_2O_3, Bi(PD)/Ga_2O_3, Pd(PD)/Ga_2O_3, and Pd-Bi(PD)/Ga_2O_3 samples in the conventional mode using secondary electron imaging (SEI) and in the compositional mode using a retractable backscattered electron imaging (RBEI) are shown in Fig. S4. Pillar-shaped Ga_2O_3 particles with a length of 1−2 μm and width of ~500 nm were observed. The morphology and particle size of Ga_2O_3 didn't change much after cocatalysts loading. The bright spots in the compositional images are assigned to the Pd cocatalyst and Pd-Bi bimetallic cocatalyst particles in the Pd(PD)/Ga_2O_3 and Pd-Bi(PD)/Ga_2O_3 samples, respectively. The particle size distribution is made as shown in Fig. S4, right side. The average particle size of the Pd cocatalyst was ~22 nm. The average particle size of Pd-Bi bimetallic nanoparticles decreased and it was ~20 nm. There were no bright spots observed in the compositional SEM images of Ga_2O_3 and Bi(PD)/Ga_2O_3 samples.

S3.4 STEM images and elemental mappings of Pd-Bi(IMP)/Ga_2O_3

The STEM image and elemental mappings of Ga, O, Pd, and Bi are shown in Fig. S5. The Pd and Bi species are dispersed on the surface of Ga_2O_3.

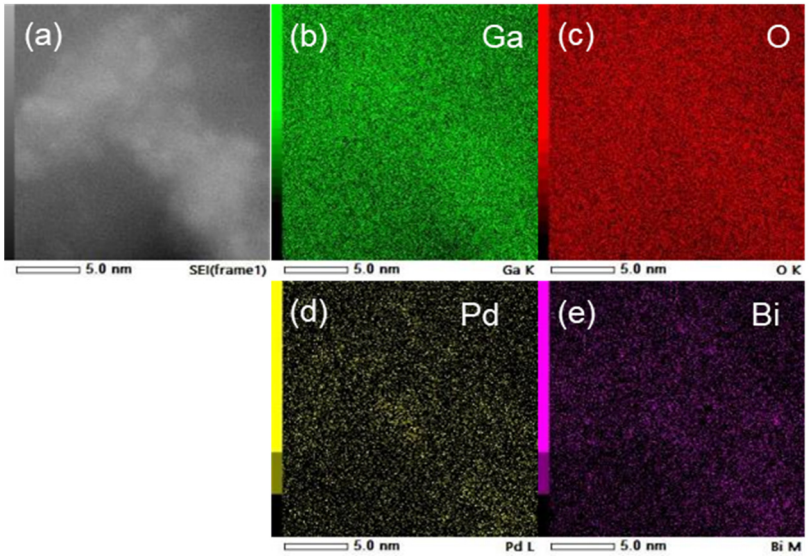

Fig. S5 (a) STEM image, and elemental mappings of (b) Ga, (c) O, (d) Pd, and (e) Bi of the Pd-Bi(IMP)/Ga_2O_3 sample.

S3.5 STEM images and elemental mappings of Pd-Bi(IMP-673R)/Ga_2O_3 sample

The STEM image and elemental mappings of the Ga, O, Pd, and Bi of the Pd-Bi(IMP-673R)/Ga_2O_3 sample are shown in Fig. S6. Pd and Bi species are dispersed on the surface of Ga_2O_3.

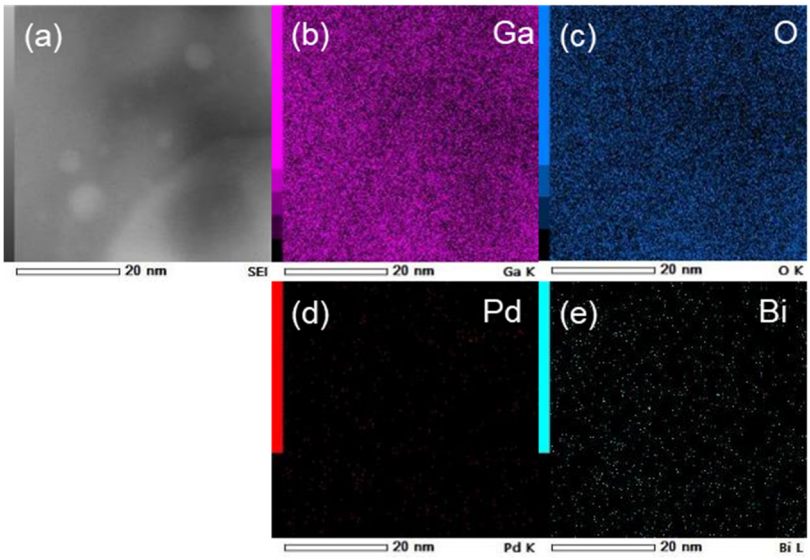

Fig. S6 (a) STEM image, and elemental mappings of (b) Ga, (c) O, (d) Pd, and (e) Bi for the Pd-Bi(IMP-673R)/Ga_2O_3 sample.

S3.6 STEM images and elemental mappings of Pd-Bi(IMP-973R)/Ga_2O_3 sample

The STEM image and elemental mappings of the Ga, O, Pd, and Bi for the Pd-Bi(IMP-973R)/Ga_2O_3 sample are shown in Fig. S7. No formation of aggregate is observed even at a high temperature of 973 K.

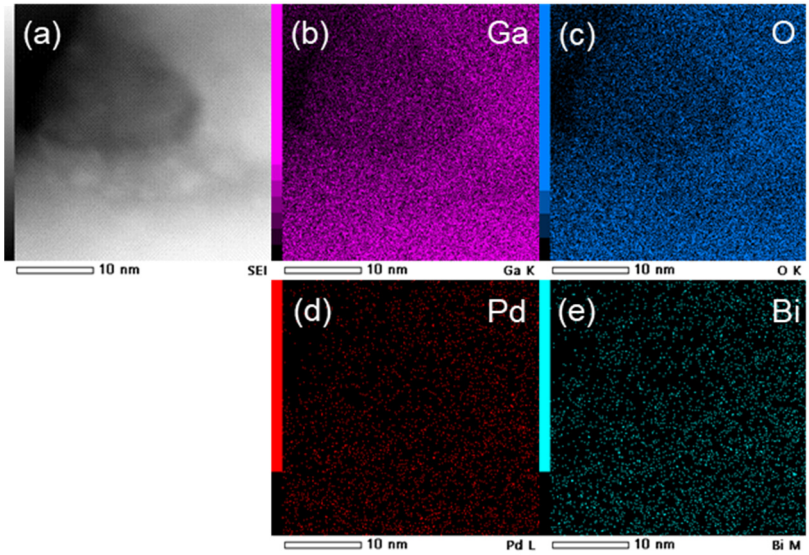

Fig. S7 (a) STEM image, and elemental mappings of (b) Ga, (c) O, (d) Pd, (e) Bi for the Pd-Bi(IMP-973R)/Ga_2O_3 sample.

S3.7 XAFS of Pd_3Bi/SiO_2 catalyst

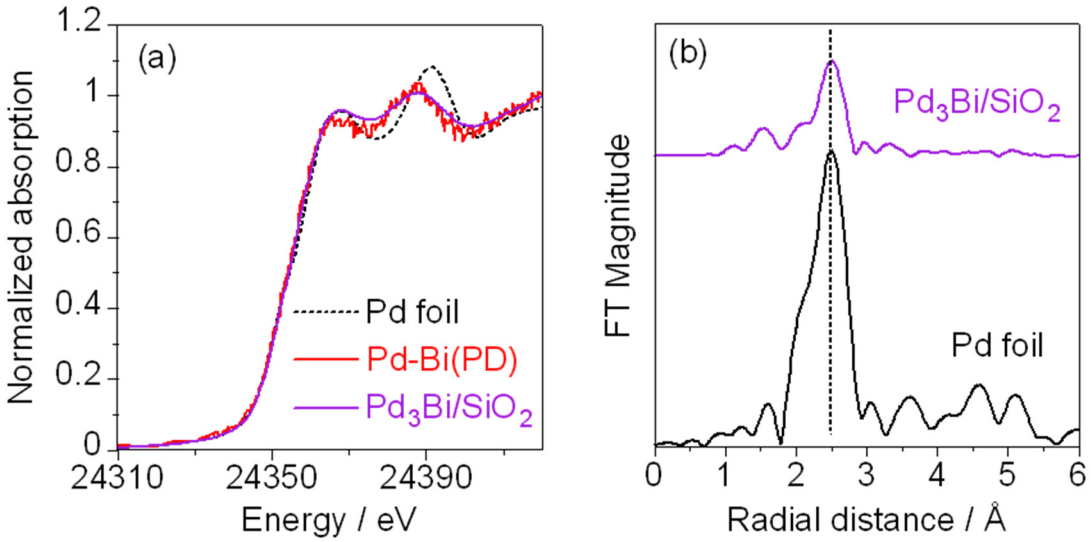

Fig. S8 a) XANES and b) FT EXAFS spectra of Pd_3Bi/SiO_2. The Pd and Bi loading amounts were 2.0 wt.% each for preparing Pd_3Bi/SiO_2.

S3.8 XRD pattern of Pd_3Bi/SiO_2 catalyst

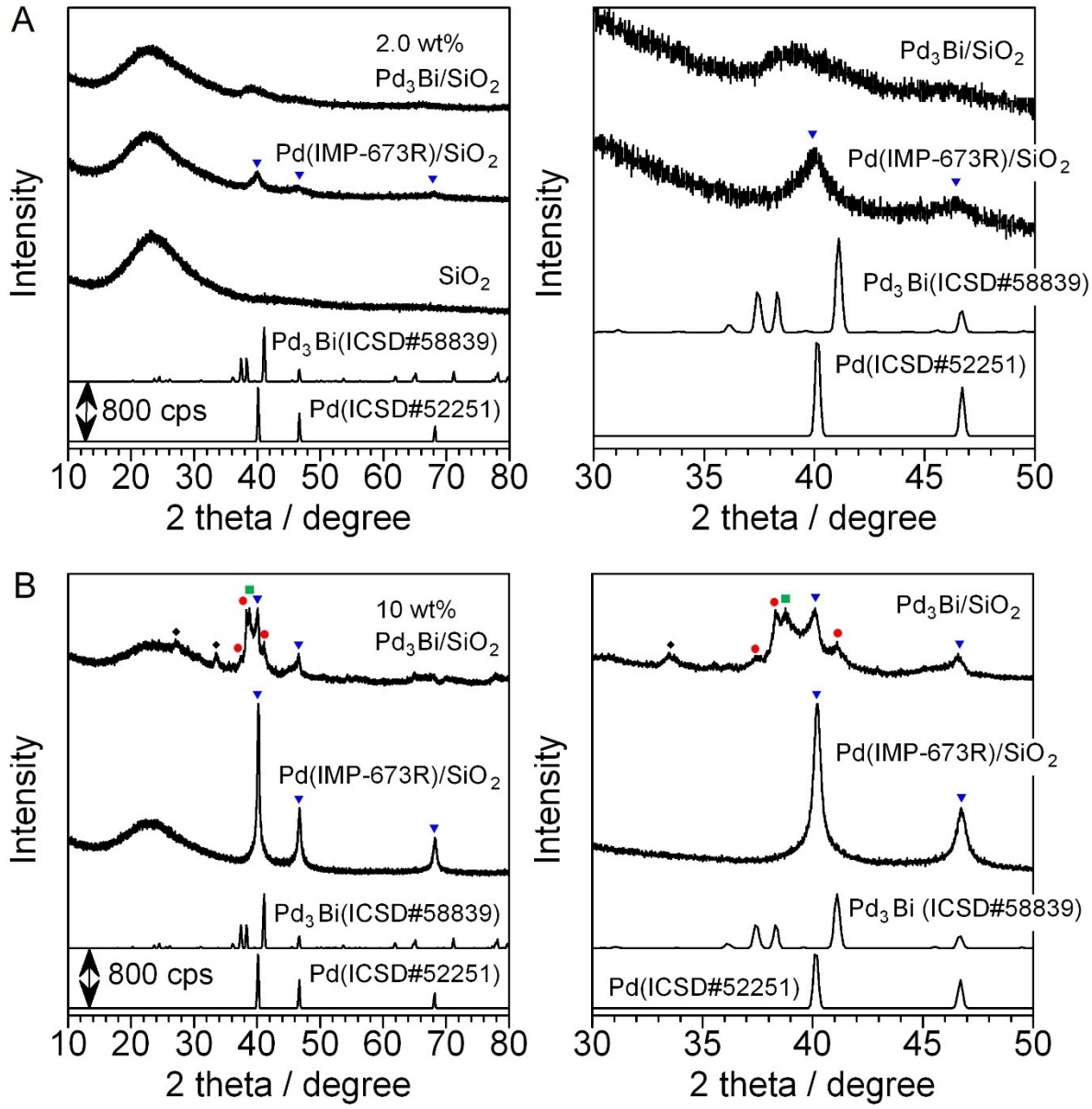

Fig. S9 XRD patterns of Pd_3Bi/SiO_2, Pd(IMP-673R)/SiO_2, SiO_2 and, references. (A) loading amount of each Pd and Bi was 2.0 wt.%, and (B) loading amount of each Pd and Bi was 10 wt.%. Symbols: circle = Pd_3Bi (ICSD#58839), triangle = Pd (ICSD#52251), diamond = α-Bi_2O_3 (ICSD#15072), square = Pd_2Si (ICSD#43209).

In the XRD pattern of the Pd_3Bi/SiO_2 sample (Fig. S9 A), distinct broad lines were observed due to the low loading amount of Pd and Bi (2 wt.% for each). We prepared the Pd_3Bi/SiO_2 with a high loading amount of Pd and Bi (10 wt.% for each) and measured the XRD patterns (Fig. S9 B). The lines corresponding to the Pd_3Bi phase can be seen clearly (red circles). In addition, the lines corresponding to the α-Bi_2O_3 phase (black diamonds) and Pd_2Bi phase (green square) were also observed.

S3.9 SEM image of Pd_3Bi/SiO_2 catalyst

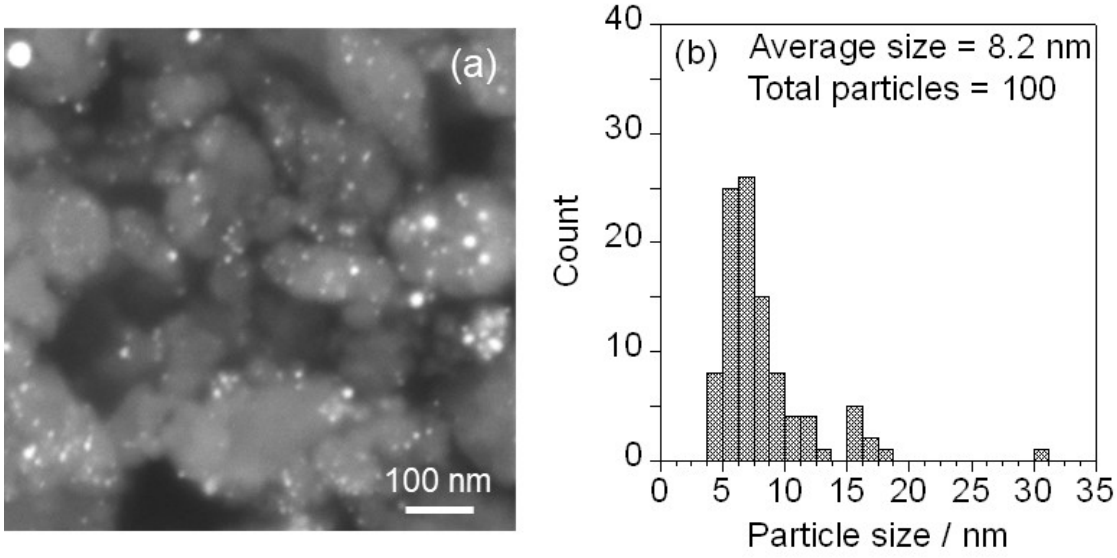

Fig. S10 a) Compositional SEM image and b) particle size distribution of Pd_3Bi/SiO_2 sample. The loading amount of Pd and Bi each was 2 wt.%.

S3.10 Properties of Pd_3Bi intermetallic compound

The crystal structure of the Pd_3Bi intermetallic compound is shown in Fig. S11.

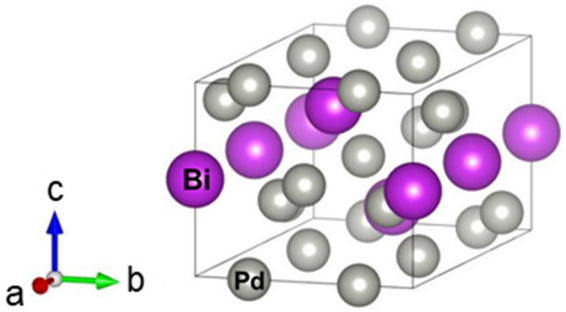

Fig. S11 Crystal structure of Pd_3Bi; Crystal system = orthorhombic, space group = Pmma, a = 9.393 Å, b = 5.752 Å, c = 4.954 Å, $\alpha = \beta = \gamma = 90°$. Pd−Pd bond length is 2.87 Å with a coordination number of 8, while Pd−Bi bond length is 2.86 Å with a coordination number of 4.

S3.11 XAFS of Pd-Bi(IMP)/Ga_2O_3 samples

XANES spectra of Pd foil, PdO, Pd-Bi(IMP)/Ga_2O_3, Pd-Bi(IMP-673R)/Ga_2O_3, and Pd-Bi(IMP-973R)/Ga_2O_3 samples are shown in Fig. S12.

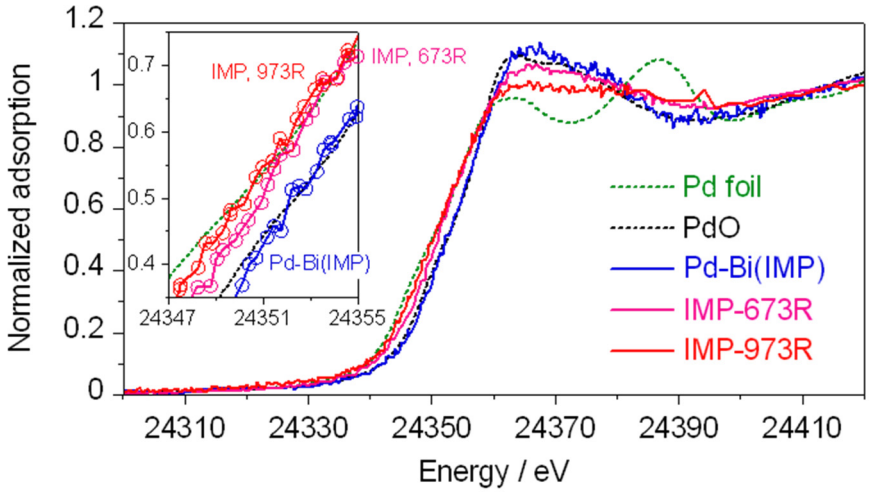

Fig. S12 Pd K-edge XANES spectra of Pd-Bi(IMP)/Ga_2O_3 and Pd-Bi(IMP-*t*R)/Ga_2O_3 samples.

S3.12 DR UV-vis spectra

The DR UV-vis spectra of the used Ga_2O_3, Bi(PD)/Ga_2O_3, Pd(PD)/Ga_2O_3, and Pd-Bi(PD)/Ga_2O_3 samples are shown in Fig. S13.

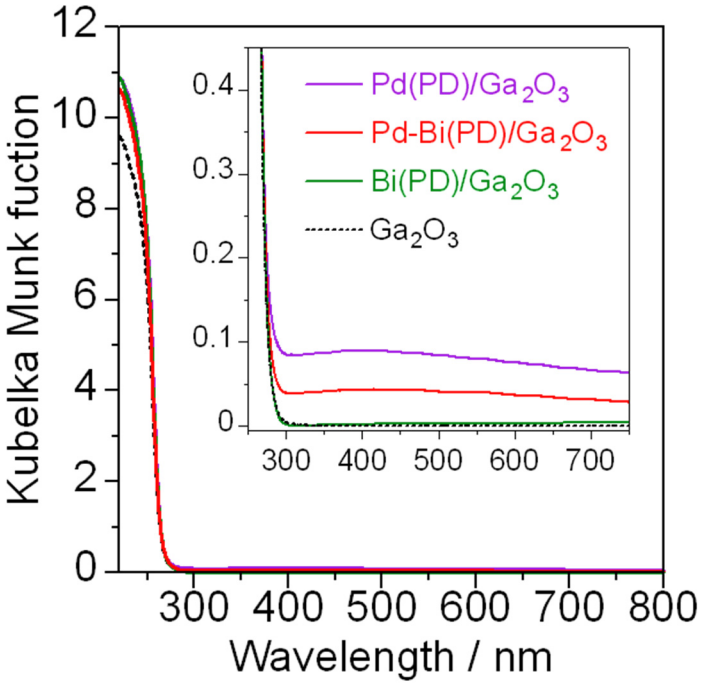

Fig. S13 DR UV-vis spectra of Ga_2O_3, Bi(PD)/Ga_2O_3, Pd(PD)/Ga_2O_3, and Pd-Bi(PD)/Ga_2O_3 samples.

S3.13 ESR spectra

In our previous study (*Energy Fuels* 2022, 36, 5393−5402), •OH formation was analysed by ESR technique with DMPO as a spin-trapping agent. We observed a direct correlation between higher •OH concentration and increased ethane selectivity. ESR spectra of the photocatalyst samples in DMPO aqueous solution were measured under UV irradiation (Fig. S14). The •OH concentration in Pd(0.1)-Bi(0.2)(PD)/Ga_2O_3 was higher than that in Pd(0.1)(PD)/Ga_2O_3. Thus, in the present case also, the enhanced ethane selectivity is related to the increase in the •OH concentration over Pd-Bi(PD)/Ga_2O_3 photocatalyst.

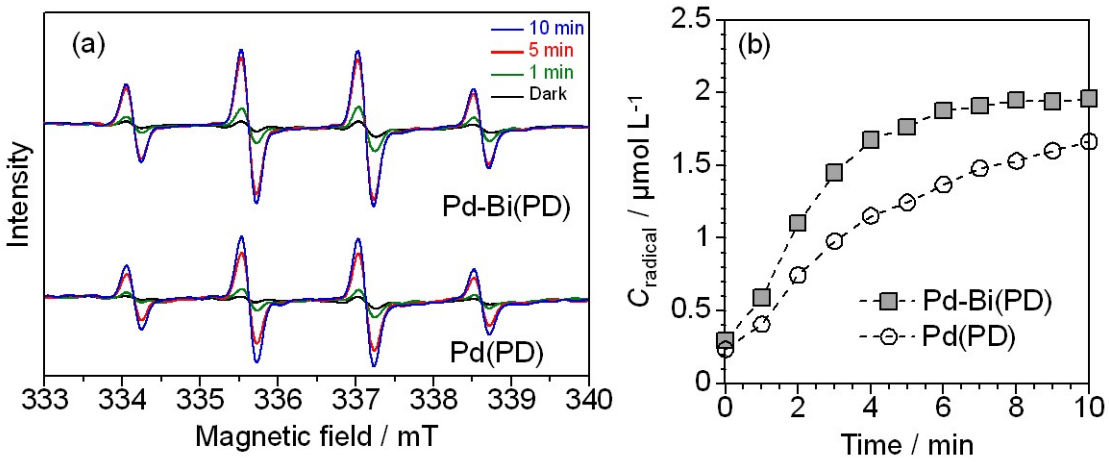

Fig. S14 (a) in-situ ESR spectra in the presence of DMPO and (b) time course of •DMPO-OH generation for Pd(PD)/Ga_2O_3, and Pd-Bi(PD)/Ga_2O_3 samples under UV irradiation.

S4. Results of reaction tests

S4.1 Results of reaction tests

The production rates and the ratio of consumed electrons and holes in the reaction are given in Table S2. The h^+/e^- value was slightly less than 1. In the case of Ga_2O_3, this was due to the error in the estimation of the low amount of products while in other cases, a small amount of carbon might be formed (*J. Catal.*, 2021, **397**, 192–200).

Table S2 Results of reaction test of photocatalytic methane conversion with water vapour over various samples

Entry	Photocatalyst	Production rate[a] / μmol min^{-1}						h^+/e^-
		H_2	C_2H_6	C_2H_4	C_3H_8	CO_2	CO	
1	Ga_2O_3	0.13	0.002	0	0	0.02	0.010	0.80
2	Pd(PD)/Ga_2O_3	1.94	0.41	0.010	0.005	0.35	0.011	0.96
3	Pd-Bi(PD)/Ga_2O_3	1.00	0.44	0.007	0.009	0.12	0.009	0.94
4	Bi(PD)/Ga_2O_3	0.27	0.003	0	0.003	0.05	0.015	0.89
5	Pd-Bi(IMP)/Ga_2O_3	0.44	0.19	0.005	0.002	0.04	0.005	0.87
6	Pd-Bi(IMP-373R)/Ga_2O_3	0.54	0.25	0.005	0.002	0.05	0.003	0.89
7	Pd-Bi(IMP-473R)/Ga_2O_3	0.58	0.27	0.005	0.004	0.05	0.004	0.90
8	Pd-Bi(IMP-673R)/Ga_2O_3	0.52	0.18	0.009	0.003	0.06	0.004	0.90
9	Pd-Bi(IMP-973R)/Ga_2O_3	0.50	0.18	0.007	0.004	0.06	0.004	0.91

[a] The production rates were measured after 3 h photoirradiation.

The apparent quantum efficiencies (AQEs) for H_2 and C_2H_6 formation in the photocatalytic methane conversion with water vapour for various samples are given in Table S3.

Table S3 Apparent quantum efficiency (AQE) for H_2 and C_2H_6 formation

Entry	Photocatalyst	AQE (H_2) (%)	AQE (C_2H_6) (%)
1	Ga_2O_3	0.58	0.01
2	Pd(PD)/Ga_2O_3	8.70	1.84
3	Pd-Bi(PD)/Ga_2O_3	4.49	1.97
4	Bi(PD)/Ga_2O_3	1.21	0.01
5	Pd-Bi(IMP)/Ga_2O_3	1.97	0.85
6	Pd-Bi(IMP-373R)/Ga_2O_3	2.42	1.12
7	Pd-Bi(IMP-473R)/Ga_2O_3	2.60	1.21
8	Pd-Bi(IMP-673R)/Ga_2O_3	2.33	0.81
9	Pd-Bi(IMP-973R)/Ga_2O_3	2.24	0.81

The percentage methane conversion, yield of ethane and selectivity of various products based on carbon basis are given in Table S4.

Table S4 Percentage methane conversion, yield of ethane and the product selectivity

Entry	Photocatalyst	CH_4 conversion (%)	C_2H_6 yield / μmol g_{cat}^{-1} h^{-1}	S_{C2H6} (%)[a]	S_{CO2} (%)[a]
1	Ga_2O_3	0.004	2.4	12	60
2	Pd(PD)/Ga_2O_3	0.15	492	68	28
3	Pd-Bi(PD)/Ga_2O_3	0.13	528	84	11
4	Bi(PD)/Ga_2O_3	0.010	3.6	7	62
5	Pd-Bi(IMP)/Ga_2O_3	0.054	228	86	9
6	Pd-Bi(IMP, 373R)/Ga_2O_3	0.070	300	87	9
7	Pd-Bi(IMP, 473R)/Ga_2O_3	0.075	324	87	8
8	Pd-Bi(IMP, 673R)/Ga_2O_3	0.055	216	80	14
9	Pd-Bi(IMP, 973R)/Ga_2O_3	0.055	216	80	14

[a] Calculated from the values in Table S2.

S4.2 Time courses of product formation

The time courses of H_2, C_2H_6, CO_2 and CO formation over various samples are shown in Fig. S15.

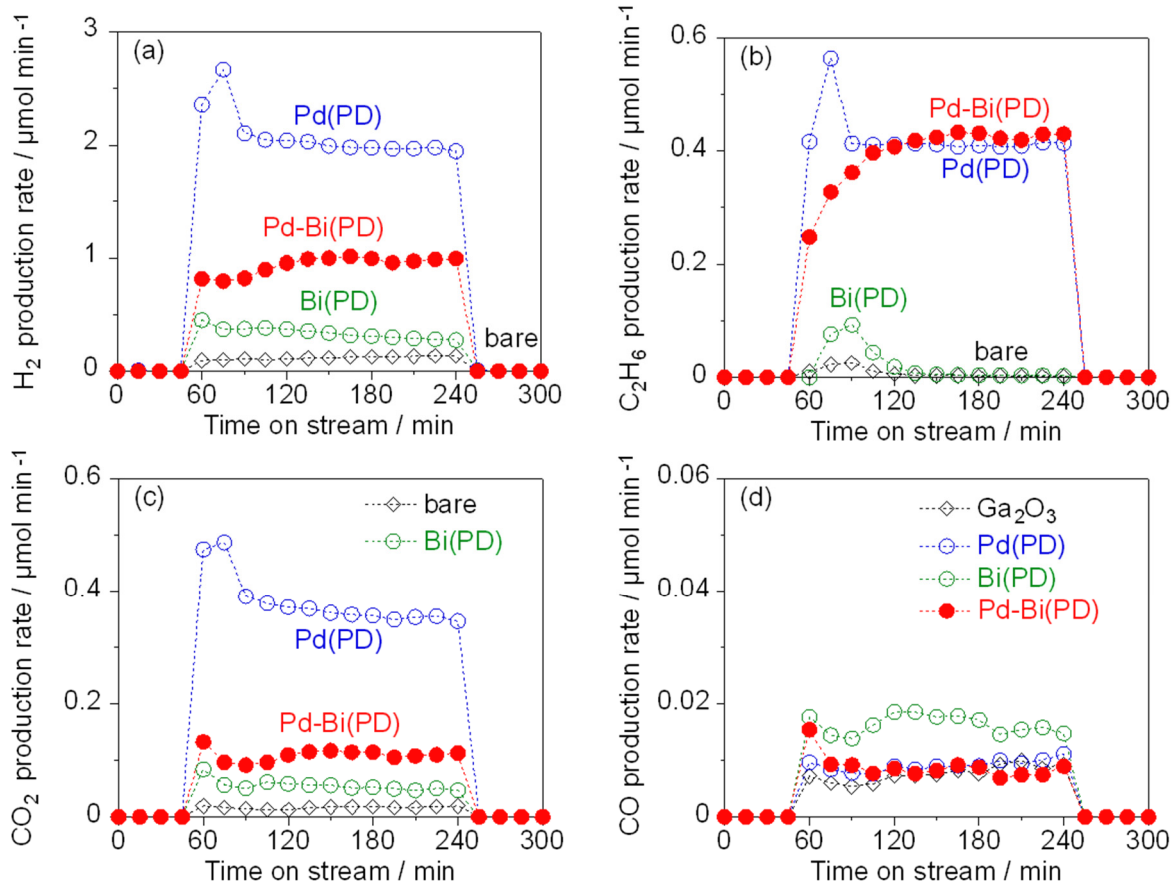

Fig. S15 Time courses of (a)H_2, (b) C_2H_6, (c) CO_2 and (d) CO formation over various samples.

S4.3 Control Experiments

The results of control experiment tests over the Pd-Bi(PD)/Ga_2O_3 samples are shown in Table S5. In the absence of CH_4, only a small amount of H_2 was produced and no other products were detected. Comparison of entry 1 and 2 shows that the products H_2, C_2H_6, C_2H_4, CO_2 and CO are derived from CH_4. In the flow of only CH_4 without water vapor (entry 3), the production rates decreased due to the absence of •OH. In the absence of any oxidants, non-oxidative coupling of methane (NOCM, $2CH_4 \rightarrow C_2H_6 + H_2$) proceeds and the production rates are generally low. However, in the present case (entry 3), small amounts of carbon oxides were also observed. This was due to the presence of adsorbed H_2O in the gas line which is very difficult to remove completely. A low value of h^+/e^- would result from the error in the estimation of the low amount of products similar to the case of Ga_2O_3.

Table S5 Results of control experiments with Pd-Bi(PD)/Ga_2O_3 photocatalyst

Entry	Reactant	Production rate[a] / μmol min^{-1}						h^+/e^-
		H_2	C_2H_6	C_2H_4	C_3H_8	CO_2	CO	
1	Ar + H_2O	0.02	0	0	0	0	-[b]	0
2	CH_4 + H_2O	1.00	0.44	0.007	0.009	0.12	0.009	0.94
3	CH_4	0.039	0.011	0	0.0005	0.002	0.001	0.67

[a] The production rates were measured after 3 h photoirradiation. [b] The peaks of Ar and CO were overlapped in the control experiment 1 and so CO production rate couldn't be analysed.